Proc. Natl. Acad. Sci. USA
Vol. 83, pp. 1179–1183, March 1986
Biochemistry

Intermediate filaments in α-keratins

(surface lattice/ionic interactions)

R. D. BRUCE FRASER*, THOMAS P. MACRAE*, DAVID A. D. PARRY†, AND EIKICHI SUZUKI*‡

*Commonwealth Scientific and Industrial Research Organization, Division of Protein Chemistry, 343 Royal Parade, Parkville, Victoria 3052, Australia; and †Department of Physics and Biophysics, Massey University, Palmerston North, New Zealand

Communicated by David R. Davies, September 27, 1985

ABSTRACT **Previous x-ray diffraction studies on the α-keratins of hair and wool have revealed that the intermediate filaments (IF) have a helical structure rendered imperfect by a precisely defined dislocation. It has also been possible to deduce a surface lattice for the IF and to determine the number of IF molecules associated with each lattice point. In this work this information is combined with data on the ionic interactions between the coiled-coil rope segments of the IF molecules to provide a plausible model for the pattern of interactions that stabilize the framework of the IF in the "hard" α-keratins. Similar interaction studies of the proteins from the IF in the so-called "soft" α-keratin from the stratum corneum layer of the skin suggest that they are likely to have an essentially similar pattern.**

Mammalian keratins may be classified into two distinct groups (1). The first of these, the so-called "hard" keratins, comprise epidermal appendages such as hair, wool, nails, and claws and contain ordered arrays of intermediate filaments (IF) embedded in a matrix of cystine-rich proteins unrelated in size or composition to the IF proteins. Other types of epithelia belong to the so-called "soft" keratin group and contain IF of a composition distinct from the hard keratin group.

The molecules in both types of α-keratin are composed of two chains of differing molecular weight and composition that have been designated types I and II (2–4). Both chains have nonhelical N-terminal and C-terminal domains and a central, coiled-coil "rod" domain (refs. 2 and 5–8; see Fig. 1 for the nomenclature used to designate the various segments). Several lines of evidence suggest that the chains are parallel in the two-strand rope segments and in axial register (3, 4, 9).

Hard keratins yield x-ray diffraction patterns of sufficient quality to permit detailed deductions to be made about the symmetry of the IF and the nature of the surface lattice (10). When combined with information now available on the chemical compositions of the IF proteins from wool (5), it is possible to devise a model for the arrangement of the coiled-coil rope segments of the IF molecules that maximizes the potential for favorable ionic interactions, subject to the constraints imposed by the lattice.

Interaction Studies

Since x-ray diffraction studies suggest that the coiled-coil rope segments form the framework of the IF (11, 12), an assessment of lateral interactions between segments in different molecules in the framework may reveal details of the modes of packing. Thus, by using a method similar to that devised by Miller and colleagues (13) attention was focused on the major segments, 1B and 2 (Fig. 1), and scores were calculated for ionic interactions, hydrophobic interactions, and hydrogen bonds for all possible combinations of relative direction and stagger. However, it was only for ionic interactions that major peaks were found. Since ionic interactions are believed to play a key part in determining the mutual alignment and registration of molecules during filament and fibril formation (14) attention was concentrated on these interactions as the likely determinants of the "docking" pattern, although it is recognized that in the final stages of assembly hydrophobic and hydrogen bond interactions will play a major stabilizing role.

The sequences of segments 1B and 2 (Fig. 1) were aligned in various ways (Fig. 2) at arbitrarily defined positions of zero stagger, and counts were made of the number of possible interactions between negatively charged residues (aspartic acid, glutamic acid) and positively charged residues (arginine, histidine, lysine) located within the axial range of ±1 residue. This process was repeated for the complete range of possible staggers for every combination of segments and the scores recorded.

The significance of a particular score compared with the expectation for a random distribution of the same selection of charged residues at a particular overlap was assessed by using a method developed by Trajstman and Lucas (15). In this method random allocations of the charged residues in the overlap zone are generated for each molecule and interaction scores are accumulated. After a sufficient number of trials a distribution curve is obtained from which any desired quantile can be extracted. In the present study the score corresponding to the 0.975 quantile for random distributions was selected as a test of significance.

In discussing the results it is convenient to specify relative axial stagger in terms of a variable Δz (Fig. 2) and to designate the type of interaction by the addition of (1BU, 1BU), (1BU, 1BD), (2U, 2U), (2U, 2D), (1BU, 2U), (1BU, 2D) as appropriate, where U (up) and D (down) are used to distinguish the direction of progression from the N-terminal to the C-terminal residue of the segment (Fig. 2). Interaction scores and 0.975 quantiles for random distributions were determined for (*i*) a typical hard keratin, a wool IF molecule composed of one chain of component 8c-1 (type 1) and one of component 7c (type II) (5), and (*ii*) a typical soft keratin, a mouse epidermal IF molecule composed of one chain of the M59K component (type I) and one chain of the M67K component (type II) (4, 7, 16).

In every case the interaction score passed through a series of maxima as the stagger was varied and many were found to exceed the 0.975 quantile. Successive maxima tended to be spaced at intervals of approximately 9- to 10-residue translations and this is clearly related to the previously reported periodic distributions of this spacing in the positively and negatively charged residues (5, 9, 17). The results obtained for segment interactions in the hard α-keratin IF protein

The publication costs of this article were defrayed in part by page charge payment. This article must therefore be hereby marked "*advertisement*" in accordance with 18 U.S.C. §1734 solely to indicate this fact.

Abbreviation: IF, intermediate filament(s).
‡Deceased September 17, 1985.

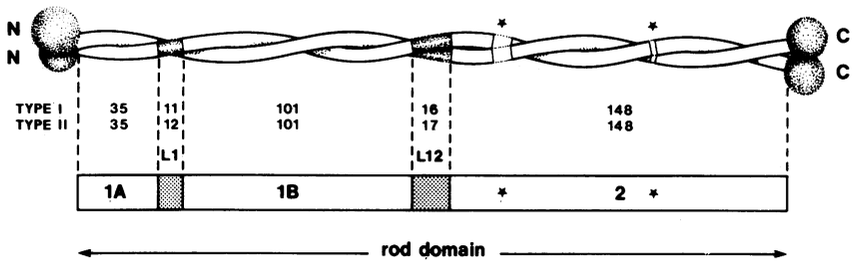

FIG. 1. The α-keratin IF molecule is composed of a type I and a type II chain and each has a central domain that is predominantly α-helical. The α-helices coil around one another to form segments of two-strand coiled-coil rope (1A, 1B, 2) that are linked by short nonhelical segments (L1, L12). The heptapeptide pattern in segment 2 is interrupted twice (*) and the regularity of the rope is disturbed at these points. The numbers of residues in the rod domain are indicated.

molecule from wool were found to be very similar to those for the protein molecule from the soft keratin of epidermis.

The number of interaction maxima that exceed the 0.975 quantile is too large to provide a satisfactory basis for developing a model of the coiled-coil framework of IF but a number of constraints can be applied, based on x-ray diffraction studies, and these are discussed in the next sections.

The Surface Lattice in α-Keratin IF

In most hard α-keratins the IF are aligned parallel to some unique direction and their x-ray diffraction patterns yield information about the helical symmetry (10–12) and the lateral dimensions (18) of the IF. The basic helix has a unit height of $h = 470$ Å and a unit twist of magnitude $|t| = 49°$ (12).

The meridional diffraction pattern, however, shows an unusual feature in that many of the orders of 470 Å are weak or absent. This was shown to be explicable in terms of a structure, which, when projected onto the fiber axis, consisted of finite sets of repeating units spaced at 198 Å intervals laid down at intervals of 470 Å (10). The number of repeating units in the set was estimated to be 7.2 ± 0.8 for point-like units and 8.6 ± 0.5 for units with an extended electron-density distribution. Neither 7 nor 8 repeats of 198 Å produce an integral multiple of 470 Å and it was concluded that the surface lattice contained a dislocation along the basic helix, as shown in Fig. 3 *a* and *b*. It will be seen that the magnitude of the dislocation is very much smaller in the case of 7 repeats, and for this reason the lattice structure shown in Fig. 3*a* was favored in our earlier studies. In both the 7- and 8-repeat models the surface lattice is conveniently defined by lattice vectors **a** and **b** (Fig. 3) and in both cases the axially projected lengths are $z_a = 74.2$ Å and $z_b = 197.9$ Å. The hand of the basic helix cannot be determined from the presently available x-ray diffraction data, and mirror images of Fig. 3 *a* and *b* would be equally acceptable. The choice used here is based on the electron microscope studies of Milam and Erickson (23), which suggest that a banding pattern of

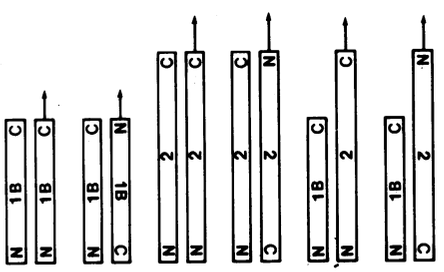

FIG. 2. The six possible interactions of the major coiled-coil segments are designated (1BU, 1BU), (1BU, 1BD), (2U, 2U), (2U, 2D), (1BU, 2U), (1BU, 2D). The pairs of segments are depicted in the position defined as zero stagger and the arrows indicate the directions defining positive stagger.

periodicity 220 Å in soft α-keratin IF is inclined in the same sense as that shown in Fig. 3 *a* and *b*. The calculated value for z_d is 217 Å for the 7-repeat model and 216 Å for the 8-repeat model (24).

The Nature of the Repeating Unit

The mean axial translation per repeating unit in the 7-repeat model is 67.1 Å and in the 8-repeat model is 58.8 Å. The filament diameter in hard α-keratin in the dry state has been estimated to be 74.5 Å (18) and, assuming a density of 1.3 $g \cdot cm^{-3}$ (25), this leads to estimates of 229 kDa and 201 kDa, respectively, for the mass associated with each repeating unit. Since the mass of the molecule in the IF of wool is around 108 kDa (5) it follows that there must be two molecules per unit cell. Steven *et al.* (19, 20) obtained estimates of the linear mass distribution in IF using scanning transmission electron microscopy (STEM) and quote a mean value of 0.067 ± 0.003 chains per Å. The values calculated for our 7- and 8-repeat models are 0.060 and 0.068 chains per Å, respectively. Thus, the 8-repeat model gives a better correspondence to the STEM value. We have suggested earlier (10) that the 7-repeat model could have a centrally located additional subfilament (Fig. 3*a*), which would raise the value to 0.068 chains per Å, giving better agreement with the STEM value.

There is some evidence, based on studies of the $\alpha \rightarrow \beta$ transformation that occurs when α-keratin is stretched, that oppositely directed chains occur in the native IF (26). Since the two chains in the molecule are known to be parallel (3) this implies that the two molecules in the repeating unit are oppositely directed (5, 10) and we make the plausible assumption that they are equivalently related with regard to their interacting surfaces. Thus, we assume that the two molecules are at least quasi-equivalently related by a diad perpendicular to the fiber axis.

Combination of Interaction and Lattice Data

Studies of helix-rich particles isolated from partial hydrolysates of wool IF indicate that strong association exists between the 1B segments of neighboring molecules (27), and the arguments presented in the previous section suggest that the interaction is most likely to be of the (1BU, 1BD) variety. If the pair of molecules associated by means of this interaction are symmetrically disposed about the lattice point at $z = 0$ (Fig. 4*a*), there are five potential interactions with the coiled-coil rope segments in the next turn of the basic helix and these are labeled a–e.

The number of possible combinations of interaction maxima is extremely large but by imposing the following plausible constraints the number can be greatly reduced. We assume (*i*) that each molecule is involved in similar sets of interactions so that the bonding is isologous, (*ii*) that the staggers between segments correspond to interaction maxima that exceed the

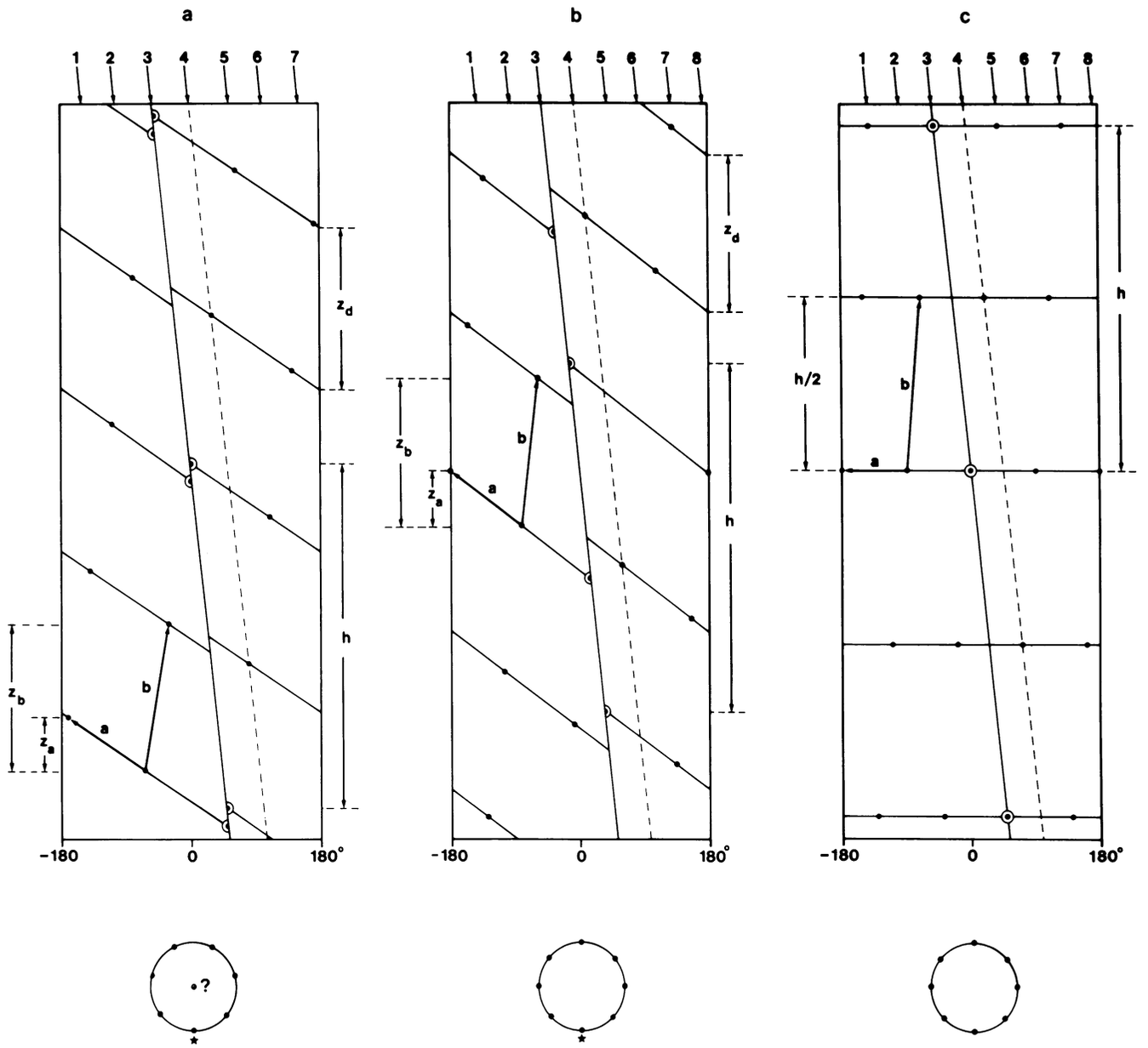

FIG. 3. (*a*) Upper: radial projection of the α-keratin IF surface lattice based on seven repeating units per h = 470 Å. Lattice vectors **a** and **b** have axial projections of z_a = 74.2 Å and z_b = 197.9 Å, respectively. When wrapped around a cylindrical surface the lattice does not form continuous helices, and the dislocation is indicated by a full line. The filament may be regarded as being made up of seven subfilaments, as indicated by arrows at the top of the diagram. The broken line identifies one of the subfilaments and repeating units occur at intervals of h = 470 Å. There is a stagger of z_b = 197.9 Å between adjacent subfilaments. The filament has true helical symmetry with a basic helix of pitch P = −3447 Å, a unit height of h = 470 Å, and a unit twist t = −49.1° (12). Lower: helical projection down the basic helix, emphasizing the seven-subfilament nature of the model. Better agreement with linear mass estimates (19, 20) is obtained if an additional, central, subfilament is incorporated. (*b*) As in *a* except that the lattice is based on eight repeating units per 470 Å. Excellent agreement with linear mass estimates (19, 20) is obtained without the need to include a central subfilament as in *a*. (*c*) Increasing z_b in *b* to $h/2$ results in a banding pattern perpendicular to the filament axis (21, 22). The basic helix now lies along the lattice vector **b** and there is a 4-fold rotation axis coincident with the filament axis.

0.975 quantile, (*iii*) that the predicted axial displacement between consecutive lattice points along the basic helix, calculated by summing the staggers of the segments in an appropriate vectorial manner, must be close to the value deduced from x-ray diffraction studies, and (*iv*) that the length of the linkage L12 between segments 1B and 2 must be stereochemically feasible, having regard to the number of residues (Fig. 1) and the limiting axial translation per residue of about 3.4 Å.

Eight types of possible isologous interaction patterns along the basic helix were investigated in the present study and these are listed in Table 1. Although the first four (f–i) may occur in the α-keratin IF they do not provide structural integrity between consecutive turns of the basic helix since no mixed segment 1B and segment 2 interactions are involved (Fig. 4*a*). For each of the remaining four isologous bonding patterns all possible combinations of interaction maxima that predicted the observed value of z_a to within ±2 residue translations and gave acceptable values for the mean residue translation in the link between segments 1B and 2 were ranked according to interaction score. The highest ranking combinations are given in the upper part of Table 2 and the pattern with maximum score is illustrated in Fig. 4*b*. This pattern exhibits the observed association between 1B segments (27) and also involves associations between pairs of antiparallel molecules that are approximately in register. This is consistent with a known form of *in vitro* association that leads to particles about 480 Å in length (21, 22, 28). The mean

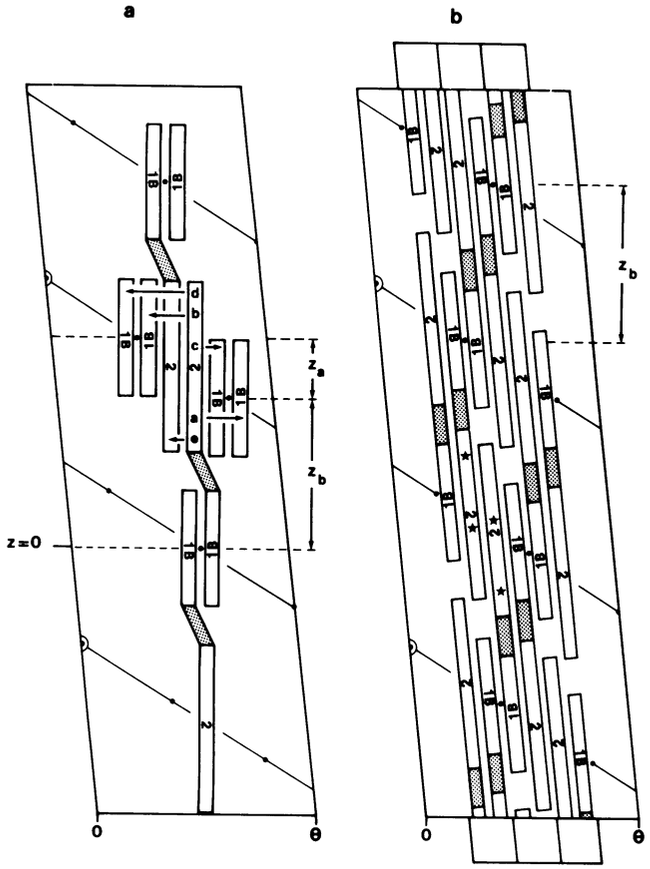

FIG. 4. (*a*) Helical projection of a portion of the surface lattice of α-keratin IF (θ is 257° and 225° for the seven- and eight-subfilament models, respectively). A repeating unit (10) is shown centered around the lattice point at $z = 0$. The nonhelical segment L12 (shaded) links coiled-coil segments in adjacent bands. Five possible associations (a–e) are considered for the interaction of segment 2 with segments in the adjacent band. (*b*) Disposition of major rod-domain segments consistent with the values of z_a and z_b in hard α-keratin and that maximizes the ionic interaction score. L12 has an average axial rise close to that observed in the β-conformation. The pattern accounts in a natural way for the observed 1B–1B interaction (27) and for two-molecule aggregates with a length around 480 Å (21, 22, 28). Interruptions in the coiled-coil regularity in segment 2 are indicated by asterisks.

axial translation per residue in the link between segments 1B and 2 for this pattern is close to that found in the β-conformation so that the chains are almost fully extended. The precise ranking of this pattern depends upon the tolerance placed on the calculated values of Δz. For example, a tolerance of ±1 brings the second listed solution into equal first ranking. The incorporation of z(1BU, 2D) = −45 rather than −34 would bring the two linking segments into register.

Table 1. Possible patterns of isologous interactions between coiled-coil rope segments along the inclined bands in α-keratin IF

Lattice point at $z = z_a$ ↓	Lattice point at $z = 0$ ↓	Designation	Interactions between coiled-coil rope segments*
1BU–1BD	1BU–1BD	f	
1BD–1BU	1BD–1BU	g	
2U–2D	2U–2D	h	
2D–2U	2D–2U	i	
1BU–1BD–2D–2U–1BU–1BD		j	a, e
1BD–1BU–2U–2D–1BD–1BU		k	b, e
1BD–1BU–2D–2U–1BD–1BU		l	c, e
1BU–1BD–2U–2D–1BU–1BD		m	d, e

*See Fig. 4*a*.

The two highest ranking solutions in the upper part of Table 2 have the general form shown in Fig. 4*b*, in which the IF may be thought of as built up from subfilaments formed by the end-to-end aggregation of pairs of antiparallel molecules in approximate register, spaced at intervals of 470 Å. Three such subfilaments are shown in Fig. 4*b*. The stagger between adjacent subfilaments is z_b and we note that if z_b was made equal to $h/2$ in the 8-repeat model a structure similar to that suggested for desmin by Geisler *et al.* (21) and for vimentin by Ip *et al.* (22) would be obtained (Fig. 3*c*). The fact that the banding appears to be perpendicular to the filament axis in some IF and inclined in others may simply be the difference between the case $z_b = h/2$ (Fig. 3*c*) and $z_b = h/2$ (Fig. 3 *a* and *b*), respectively. An additional point of interest is that the molecules are aligned parallel to the dislocation in the lattice, and so minimization of the extent of the dislocation is probably not a valid reason for preferring the 7-repeat over the 8-repeat model as was originally supposed (10).

The molecule in wool IF contains a number of cysteine residues (1, 5) that, in the native state, are paired with other cysteine residues in the fiber to form disulfide linkages. It is not known which of these linkages stabilize the IF and which link the IF to the matrix proteins but it is of interest to explore the potential for linkages between the rod domains of IF molecules in the same way as that used for exploring ionic interactions. The tolerance to be placed on the position in the sequence for any particular stagger between two segments is, from stereochemical considerations, probably ±1 residue, but for the sake of completeness we have also calculated scores for a tolerance of ±2 residues. The potential for disulfide bond formation between segments in the bonding patterns of high ionic interaction score is recorded in the upper part of Table 2 and it will be seen that the pattern of highest ionic interaction score also provides the greatest potential for stabilization through disulfide bond formation.

It is interesting to note that the combination of intersegment staggers that maximizes the potential for ionic interactions and disulfide bond formation also brings one of the heptad pattern interruptions in segment 2 into close axial register with its counterpart in a symmetry-related segment (Fig. 4*b*). The second interruption is aligned with the point at which the C-terminal nonhelical segments emerge from segment 2. Interactions between segment 1A (Fig. 1) and the longer segments is not crucial to the structural integrity of the IF according to the pattern shown in Fig. 4*b*, but such interactions may well provide additional stabilization. We have no basis, however, for speculating on the disposition of segment 1A in the filament.

Although the IF surface lattice in soft α-keratin is not known, we have carried out a similar analysis of ionic interactions assuming that z_a (Fig. 3 *a* and *b*) has the same value as in hard α-keratin (lower part of Table 2). The pattern yielding the maximum score for the soft keratin is the same as that for the hard keratin.

Conclusions

The present study has demonstrated that it is possible to find patterns of ionic interaction between the coiled-coil rope segments in the α-keratin IF proteins that are consistent with the surface lattice derived from x-ray diffraction studies. It must be emphasized that the method used to arrive at the patterns relates to potential for interaction rather than actual interaction and serves only to focus attention on potential solutions to the problem. In addition, we have not addressed the problem of the precise spatial positions (radius, azimuth) of the various segments and subsegments.

Table 2. Combinations of ionic interaction maxima between coiled-coil rope segments in wool IF protein (component 8c-1 + component 7c) and mouse epidermal IF protein (M59K + M67K), which are compatible with the observed value of z_a observed in hard keratins (Fig. 3 *a* and *b*)

Interaction pattern (Table 1)	Stagger Δz* (1BU, 1BD)	(2U, 2D)	(1BU, 2U)	(1BU, 2D)	Calculated Δz_a*	Ionic score	$\langle h_{12} \rangle$,† Å	SS bonding‡ ±1	±2	Ranking
				Wool keratin						
l	14	13	—	−34	48	182	3.18	6	10	1
	15	13	—	−34	49	176	3.23	6	10	
	16	13	—	−34	50	176	3.27	6	10	
l	−5	13	—	−45	51	176	2.30	2	8	2
	−5	12	—	−45	50	170	2.34	2	4	
l	4	4	—	−45	51	172	3.13	0	4	3a
	5	4	—	−45	50	170	3.18	0	2	
l	−5	32	—	−34	49	172	1.42	7	7	3b
l	−5	−7	—	−54	49	170	3.23	0	1	4
k	−5	4	−53	—	50	172	2.72	0	0	3c
k	4	13	−53	—	50	172	2.72	2	8	3d
				Epidermal keratin						
l	14	13	—	−34	48	172	3.18			1
	14	15	—	−34	50	168	3.09			
l	−16	43	—	−34	48	168	0.39			2
	−15	43	—	−34	49	164	0.44			
	−16	43	—	−35	50	156	0.39			
l	4	4	—	−45	51	166	3.13			3a
	4	3	—	−45	50	160	3.18			
l	−16	4	—	−54	49	166	2.20			3b
	−15	4	—	−54	50	162	2.25			
l	−5	13	—	−45	51	162	2.30			5
k	−5	4	−53	—	50	164	2.71			4a
k	4	13	−53	—	50	164	2.71			4b

The interaction patterns are defined in Table 1 and the staggers are given in Fig. 2.
*Expressed in residue translations of 1.485 Å, appropriate to the coiled-coil conformation. The target value for Δz_a is 49.9.
†$\langle h_{12} \rangle$ is the mean axial translation per residue in the nonhelical segment linking coiled-coil rope segments 1B and 2.
‡The potential number of disulfide linkages between the coiled-coil rope segments in a repeating unit calculated on the basis of a tolerance of ±1 and ±2 residues from exact register.

However, we have identified two possible models for the packing arrangement of the individual molecules in the IF of hard α-keratin. In both cases the basic helix is precisely defined as are the surface lattice parameters, the axial relationship between the coiled-coil rope segments, and their relationship to the banding pattern. All of these features are capable of testing by electron microscopy using specific labels and by decoration and three-dimensional reconstruction techniques similar to those that have been used with other filaments.

1. Fraser, R. D. B., MacRae, T. P. & Rogers, G. E. (1972) *Keratins: Their Composition, Structure and Biosynthesis* (Thomas, Springfield, IL).
2. Hanukoglu, I. & Fuchs, E. (1983) *Cell* **33,** 915–924.
3. Woods, E. F. & Inglis, A. S. (1984) *Int. J. Biol. Macromol.* **6,** 277–283.
4. Parry, D. A. D., Steven, A. C. & Steinert, P. M. (1985) *Biochem. Biophys. Res. Commun.* **127,** 1012–1018.
5. Crewther, W. G., Dowling, L. M., Steinert, P. M. & Parry, D. A. D. (1983) *Int. J. Biol. Macromol.* **5,** 267–274.
6. Geisler, N. & Weber, K. (1982) *EMBO J.* **1,** 1649–1656.
7. Steinert, P. M., Rice, R. H., Roop, D. R., Trus, B. L. & Steven, A. C. (1983) *Nature (London)* **302,** 794–800.
8. Crick, F. H. C. (1953) *Acta Crystallogr.* **6,** 689–697.
9. Parry, D. A. D., Crewther, W. G., Fraser, R. D. B. & MacRae, T. P. (1977) *J. Mol. Biol.* **113,** 449–454.
10. Fraser, R. D. B. & MacRae, T. P. (1983) *Biosci. Rep.* **3,** 517–525.
11. Fraser, R. D. B. & MacRae, T. P. (1973) *Polymer* **14,** 61–67.
12. Fraser, R. D. B., MacRae, T. P. & Suzuki, E. (1976) *J. Mol. Biol.* **108,** 435–452.
13. Hulmes, D. J. S., Miller, A., Parry, D. A. D., Piez, K. A. & Woodhead-Galloway, J. (1973) *J. Mol. Biol.* **79,** 137–148.
14. Fraser, R. D. B., MacRae, T. P., Suzuki, E. & Tulloch, P. A. (1981) in *Structural Aspects of Recognition and Assembly in Biological Macromolecules*, eds. Balaban, M., Sussman, J. L., Traub, W. & Yonath, A. (Balaban International Science Services, Rehovot, Israel), pp. 327–340.
15. Trajstman, A. C. & Lucas, I. (1984) *Report VT84/9* (Commonwealth Scientific and Industrial Research Organisation, Division of Mathematics and Statistics, Melbourne, Australia).
16. Steinert, P. M., Parry, D. A. D., Idler, W. W., Johnson, L. D., Steven, A. C. & Roop, D. R. (1985) *J. Biol. Chem.* **260,** 7142–7149.
17. McLachlan, A. D. & Stewart, M. (1982) *J. Mol. Biol.* **162,** 693–698.
18. Fraser, R. D. B., Gillespie, J. M. & MacRae, T. P. (1973) *Comp. Biochem. Physiol. B* **44,** 943–947.
19. Steven, A. C., Wall, J., Hainfeld, J. & Steinert, P. M. (1982) *Proc. Natl. Acad. Sci. USA* **79,** 3101–3105.
20. Steven, A. C., Hainfeld, J. F., Wall, J. S. & Steinert, P. M. (1983) *J. Cell Biol.* **97,** 1939–1944.
21. Geisler, N., Kaufmann, E. & Weber, K. (1985) *J. Mol. Biol.* **182,** 173–177.
22. Ip, W., Hartzer, M. K., Pang, S. Y. Y. & Robson, R. M. (1985) *J. Mol. Biol.* **183,** 365–375.
23. Milam, L. & Erickson, H. P. (1982) *J. Cell Biol.* **94,** 592–596.
24. Fraser, R. D. B. & MacRae, T. P. (1985) *Biosci. Rep.* **5,** 573–579.
25. Fraser, R. D. B. & MacRae, T. P. (1957) *Text. Res. J.* **27,** 867–872.
26. Fraser, R. D. B., MacRae, T. P., Parry, D. A. D. & Suzuki, E. (1969) *Polymer* **10,** 810–826.
27. Woods, E. F. & Gruen, L. C. (1981) *Aust. J. Biol. Sci.* **34,** 515–526.
28. Quinlan, R. A., Cohlberg, J. A., Schiller, D. L., Hatzfield, M. & Franke, W. W. (1984) *J. Mol. Biol.* **178,** 365–388.